



N71-17328

NASA CR-72770

FINAL REPORT

**DEVELOPMENT OF MANUFACTURING PROCESS
FOR LARGE-DIAMETER CARBON-BASE
MONOFILAMENTS BY CHEMICAL VAPOR DEPOSITION**

by

R. L. Hough

HOUGH LABORATORY

708 Rice Street

Springfield, Ohio 45505

prepared for

NATIONAL AERONAUTICS AND SPACE ADMINISTRATION

November 11, 1970

CONTRACT NAS3-12429

NASA Lewis Research Center

Cleveland, Ohio 44135

Project Managers: David L. McDanels

John P. Merutka

**CASE FILE
COPY**

NOTICE

This report was prepared as an account of Government-sponsored work. Neither the United States, nor the National Aeronautics and Space Administration (NASA), nor any person acting on behalf of NASA:

- A.) Makes any warranty or representation, expressed or implied, with respect to the accuracy, completeness, or usefulness of the information contained in this report, or that the use of any information, apparatus, method, or process disclosed in this report may not infringe privately-owned rights; or
- B.) Assumes any liabilities with respect to the use of, or for damages resulting from the use of, any information, apparatus, method or process disclosed in this report.

As used above, "person acting on behalf of NASA" includes any employee or contractor of NASA, or employee of such contractor, to the extent that such employee or contractor of NASA or employee of such contractor prepares, disseminates, or provides access to any information pursuant to his employment or contract with NASA, or his employment with such contractor.

Requests for copies of this report should be referred to

National Aeronautics and Space Administration
Scientific and Technical Information Facility
P. O. Box 33
College Park, Md. 20740

FINAL REPORT

DEVELOPMENT OF MANUFACTURING PROCESS
FOR LARGE-DIAMETER CARBON-BASE
MONOFILAMENTS BY CHEMICAL VAPOR DEPOSITION

by

R. L. Hough

HOUGH LABORATORY
708 Rice Street
Springfield, Ohio 45505

prepared for

NATIONAL AERONAUTICS AND SPACE ADMINISTRATION

November 11, 1970

CONTRACT NAS3-12429

NASA Lewis Research Center
Cleveland, Ohio 44135
Project Managers: David L. McDanel
John P. Merutka

TABLE OF CONTENTS

SECTION	PAGE
Summary	1
I. Introduction	2
II. Large Diameter Carbon Monofilament Development	7
A. Chemical Vapor Deposition	7
B. Advantages of CVD Process	7
III. Process	8
A. Equipment	8
B. Substrate	9
C. Plating Atmosphere	9
IV. Fiber Characterization	11
A. Ultimate Tensile Strength	11
B. Modulus	11
C. Density	11
D. High Temperature Tensile Strength	12
E. Structure	12
F. Composition	12
V. Results and Discussion	13
A. Tungsten Substrate	13
B. Carbon Substrate	13
C. Processing Problem Areas	20
D. Fiber Defects	26
E. Crystallographic Structure	27
F. Comparison of Properties	28
VI. Conclusions	32
References	33
Appendix	35

LIST OF ILLUSTRATIONS

Figure	Title	Page
1	Strength vs. Diameter - Selected Carbon Monofilaments- - -	3
2	Ultimate Tensile Strength vs. Elastic Modulus for Fibers and Yarns- - - - -	6
3	Typical Electrode Configuration- - - - -	10
4	Uneven Pyrolytic Graphite Growth Along Tungsten Substrate Ridges - - - - -	14
5	Smoother Pyrolytic Graphite Growth on Tungsten - - - - -	14
6	1.5 Mil (37 μ) Smooth-Surfaced Pyrolytic Graphite Fiber on on Carbon- - - - -	15
7	Telescope Fracture in Tension- - - - -	15
8	Cross-Section - Delaminated Pyrolytic Graphite on Carbon -	17
9	Carbon Deposit by Ion Bombardment- - - - -	17
10	Carbon-Alloy Fiber Surface - - - - -	18
11	Fracture Initiated at a Nodule - - - - -	19
12	SEM View of Carbon-Alloy Fracture in Bending - - - - -	21
13a	SEM View of Carbon-Alloy Tensile Fracture > 400,000 psi (276,000 N/cm ²)- - - - -	22
13b	Close-up SEM View of Figure 13a- - - - -	22
14	Strength-Diameter vs. Month for Monofilament Development -	23
15	Proposed Functional Relationship of Process Variables- - -	25
16	X-ray Diffraction Pattern for Carbon-Alloy Fiber - - - - -	29
17	Specific Strength vs. Selected Filaments - - - - -	30
18	Specific Modulus vs. Selected Filaments- - - - -	31

ABSTRACT

Research was conducted to develop large diameter carbon monofilament in the 2.0 to 10.0 mil diameter range using the chemical vapor deposition process. Monofilaments have been synthesized in the 3.0 to 4.0 mil diameter range having measured ultimate tensile strength up to 541,000 psi and an elastic modulus of 27.7×10^6 psi. The high strength filaments were synthesized by alloying the carbon with nominally 25 to 35 mole % elemental boron. Other alloying agents, silicon or aluminum, did not prove satisfactory. Unalloyed carbon fibers were relatively weak, having maximum measured tensile strengths of ca. 160,000 psi.

SUMMARY

A research program was conducted to develop large diameter carbon monofilament in the 2.0 to 10.0 mil diameter range using the chemical vapor deposition method. Monofilaments in lengths of up to 200 feet have been synthesized in the 3.0 to 4.0 mil diameter range having measured ultimate tensile strength up to 541,000 psi and an elastic modulus of 27.7×10^6 psi. The high strength filaments were synthesized by alloying the carbon with nominally 25 to 35 mole per cent elemental boron. Other alloying agents, as silicon or aluminum, did not prove satisfactory. Unalloyed carbon fibers were relatively weak, having maximum measured tensile strengths of ca. 160,000 psi.

X-ray diffraction studies performed on both alloyed and unalloyed fibers indicates that the boron exists as a highly orientated tetragonal phase within the pyrolytic carbon matrix. A broadening of the diffraction rings indicates that the carbon crystallites comprising the matrix are very small. The graphitic basal planes for the unalloyed fibers are preferentially orientated with the c-axis perpendicular to the fiber axis. An estimated 90 to 95 per cent c-axis orientation is within 22° of normal.

These filaments are synthesized by chemical vapor deposition utilizing a "hot wire" apparatus. A 1.3 mil carbon substrate is drawn through the apparatus at a rate of 0.75 fpm. Carbon is preferable over other substrates, as tungsten, since it does not react with the deposited material and, therefore, does not interfere with initial nucleation and growth of the pyrolytic fiber.

Limitations on achieving higher measured tensile strength are believed to arise from gas-phase nucleated soots which then migrate to the growing pyrolytic surface, causing defect structures. Additional research is required to further improve the unique properties of these fibers and to increase production rate.

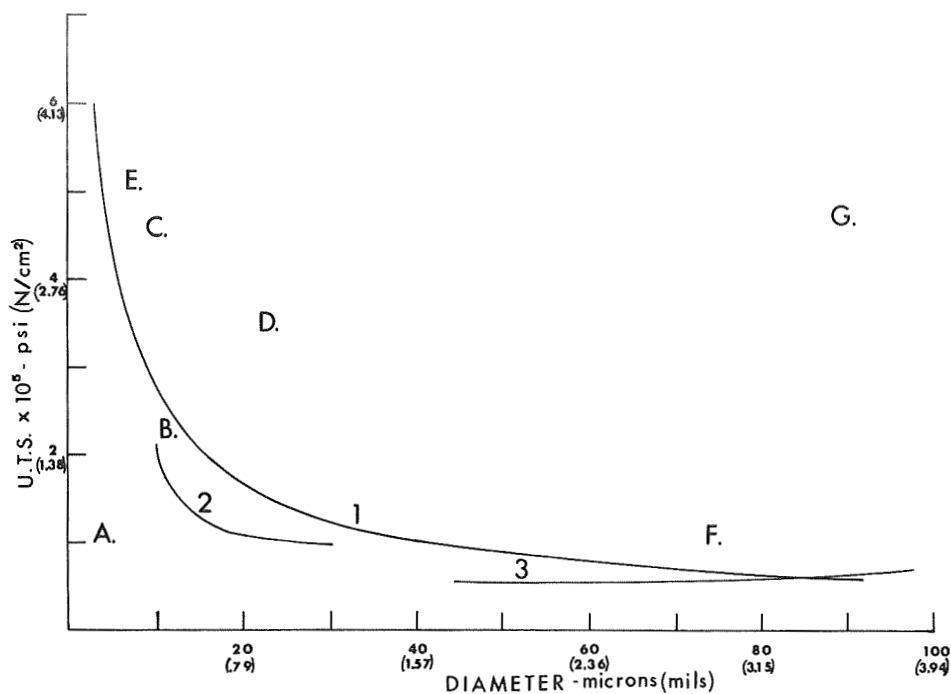
I. INTRODUCTION

The strength potential inherent in the graphitic structure was demonstrated by Bacon, who grew graphite whiskers under near-equilibrium conditions in a D. C. electric arc (Reference 1). The whisker diameters ranged from 0.02 mils to 0.2 mils (0.5μ to 5.0μ) with basal planes parallel to the fiber axis. Ultimate tensile strength of 2,800,000 psi ($1,930,000 \text{ N/cm}^2$) and modulus of nearly 140,000,000 psi ($96,400,000 \text{ N/cm}^2$) were measured for the smallest whiskers or for ribbon shaped whiskers where a large gripping surface-to-volume ratio minimized basal plane slippage. That such slippage is a limiting factor in actual measured strength is shown in Figure 1, where the point A denotes a U. T. S. value for a 0.2 mil (5.0μ) sublimed whisker (Reference 2).

The highly anisotropic nature of the near perfect graphite (i.e., the very high strength in the "a" direction and weak delamination resistance in the "c" direction) limits the practical fiber strength for larger diameter monofilaments of perfectly ordered graphite. Less highly ordered graphitic monofilaments may therefore exhibit higher measured strength because of intrinsic locking mechanisms which inhibit basal plane slippage.

M. Hillert and N. Lange grew polycrystalline graphite filaments by pyrolysis of hydrocarbons at 1832°F (1000°C) in a silica tube furnace. Bacon (Reference 1) measured the tensile strength of these fibers and found a 0.5 mil (12μ) diameter filament with U. T. S. of 220,000 psi ($152,000 \text{ N/cm}^2$). (See point B of Figure 1.)

R. G. Bourdeau (References 3 and 4) synthesized pyrolytic graphite whiskers over a wide range of diameters. These whiskers grew in the temperature range of from 1832°F to 2552°F (1000°C to 1400°C). Tensile strength vs. diameter is shown as curve no. 1 in Figure 1. Points C and D represent isolated, yet extremely interesting, values also measured by Bourdeau. The fiber with strength displayed at point C is found to have a modulus of $92,400,000 \text{ psi}$ ($63,700,000 \text{ N/cm}^2$). Unfortunately, the work of Bourdeau was never published in the open literature, nor was additional research performed. The synthesis parameters are complex, and years of research may very well be required before pyrolytic graphite whiskers are obtained having reproducible properties (Reference 5).



- | | |
|---|--|
| A. Sublimed whisker (Ref. 1) | 1. Pyrolytic graphite whiskers (Ref. 4) |
| B. Polycrystalline whisker | 2. Carbon monofilament from PVC pitch (Ref. 7) |
| C. Pyrolytic whisker ($E = 92.4 \times 10^6$ psi, 63.7×10^6 N/cm ²) | 3. Pyrolytic carbon on 25 μ (1 mil) tungsten (Ref. 10) |
| D. Pyrolytic whisker ($E = 8.7 \times 10^6$ psi, 6.0×10^6 N/cm ²) | |
| E. Stress-graphitized carbon fiber (Ref. 6) | |
| F. Pyrolytic carbon on 12 μ (0.5 mil) tungsten (Texaco) (Ref. 12) | |
| G. Carbon alloy fiber | |

Figure 1 - Strength vs. Diameter - Selected Carbon Monofilaments

Other methods for forming filamentous carbon include the stress-graphitization of rayon or other organic yarns. The result is a fine-grained, relatively disordered microstructure which never fully develops into a three-dimensional ordering. Therefore, there is no tendency for delamination. Point E in Figure 1 represents a single fiber extracted from stress-graphitized carbonized rayon yarn as measured by Bacon (Reference 6). There is apparently no information available on strength vs. diameter for larger diameter stress-graphitized carbon monofilament.

Otani (Reference 7) reports tensile strengths of nominally 100,000 psi ($68,900 \text{ N/cm}^2$) for 1.0 mil (25μ) carbon monofilament derived by pyrolysis of polyvinyl chloride pitch. His data are displayed as curve no. 2 in Figure 1. Similar strength is reported by the Great Lakes Carbon Corporation for glassy carbon monofilament having a highly cross-linked structure (Reference 8). Strengths of from below 40,000 psi ($27,600 \text{ N/cm}^2$) to nearly 150,000 psi ($103,500 \text{ N/cm}^2$) have been measured on these glassy 1.0 mil (25μ) diameter monofilaments in our laboratory.

The application of strain annealing to pyrolytic graphite will improve dimensional stability and improve physical properties unless the pyrolytic graphite structure is relatively defective. Thus, Stover and Berning (Reference 9) have demonstrated increased tensile strength for bulk strain-annealed pyrolytic graphite at both room and elevated temperatures. Because of time limitations, Bourdeau (Reference 5) did not investigate the effects of strain-annealing on the pyrolytic graphite whisker material beyond a nominal 5% elongation. Regrettably, this is not enough to produce any significant effects on strength and modulus.

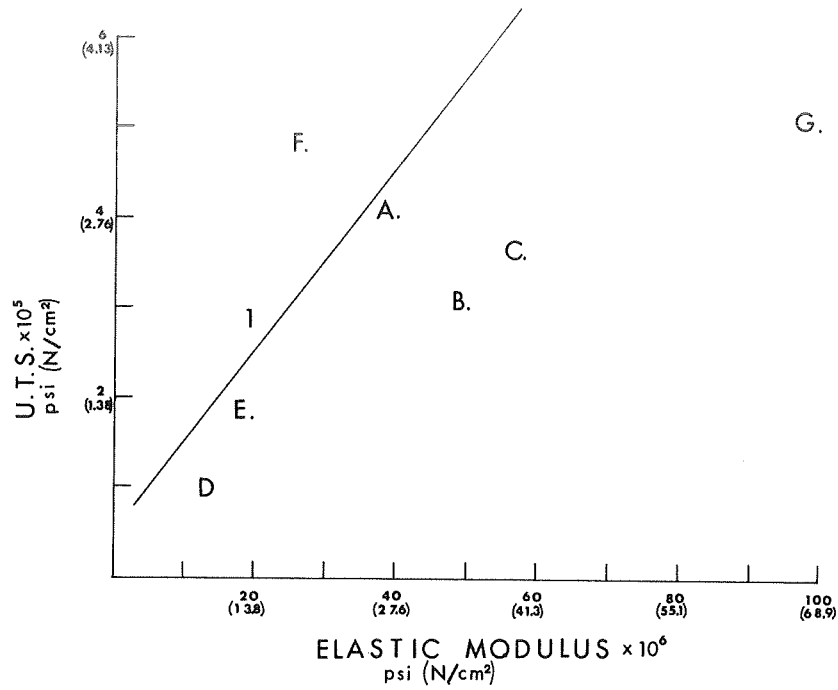
An internal program in the Plastics Branch, Nonmetallic Materials Division of the Air Force Materials Laboratory from March 1962 to July 1963 demonstrated the feasibility of forming continuous pyrolytic graphite filaments on a tungsten substrate in lengths of 2600 feet (793 meters) (Reference 10). Fiber strength vs. diameter on 1.0 mil (25μ) diameter tungsten is shown by curve no. 3 in Figure 1 (Reference 11). It was recognized that the 1.0 mil (25μ) diameter tungsten substrate was not ideal because of the weight penalty attending the high density. Also, Kirkendall voids formed between the core and the graphite layer due to the rapid diffusion of carbon into the tungsten

lattice. Thus, the core tended to contribute nothing toward mechanical properties. One-half mil (12μ) diameter tungsten was therefore considered as it would occupy less volume in the fiber and present a smaller diffusion sink. Before large diameter graphite fibers could be demonstrated utilizing the 0.5 mil (12μ) tungsten, internal research programs were redirected toward the then emerging boron fiber program. Thus, curve no. 3 in Figure 1 represents maximum strength/diameter obtained (Reference 11) before project termination.

Under company sponsored research, Texaco Experiment Inc. continued development of carbon monofilament deposited on 0.5 mil (12μ) tungsten. Three mil (76μ) diameter fiber was formed with a modulus of 18,000,000 psi ($12,400,000$ N/cm²) and tensile strength of about 100,000 psi ($68,000$ N/cm²) (Reference 12). Research and development of fibers and composites was abandoned at Texaco beginning in 1968 (Reference 13).

Carbon yarns have been commercially available since 1959. More recently, "graphite" yarns have been available. Crystallite reorientation of these yarns will increase the elastic modulus and the tensile strength. Similar reorientation by mechanical drawing produces an increased elastic modulus and tensile strength for thermoplastic polymers. Carbon yarns can be stretched at least 50 to 60 per cent under proper conditions of time, temperature, and applied force. The elastic modulus may increase from five to eight million psi ($3,445,000$ N/cm² - $5,512,000$ N/cm²) to nearly 100,000,000 psi ($68,900,000$ N/cm²). Tensile strength may go from 100,000 psi ($68,900$ N/cm²) to nearly 400,000 psi ($275,600$ N/cm²). The hot stretched carbon yarn is usually composed of discrete crystallites joined by some amorphous carbon. The precursor polymer and the effect of such pyrolysis conditions as time, temperature, and atmosphere have a pronounced effect on final properties. The crystal orientation tends to approach the more perfect ordering found in pyrolytic graphite whiskers.

Because of the method of formation, graphite fibers derived by pyrolysis of polymeric precursors will contain some defects and voids which are virtually impossible to eliminate. That this is indeed the case is documented by the fact that, although high modulus values have been observed, a corresponding increase in tensile strength has not been noted. Therefore, modulus vs. strength values (points A, B & C, Figure 2) plotted for these fibers fall



- A. Courtaulds (HT) yarn
- B. Thornel 50 yarn
- C. Courtaulds (HM) yarn
- D. Pyrolytic graphite on tungsten
- E. Pyrolytic graphite on carbon
- F. Carbon alloy monofilament
- G. Thornel 100 yarn
- I. Pyrolytic Graphite Whiskers

Figure 2 - Ultimate Tensile Strength vs. Elastic Modulus
for Fibers and Yarns

below the plotted curve for pyrolytic graphite whiskers. The pyrolytic graphite whiskers themselves contain some voids and defects since measured values for the perfect graphite whisker crystals synthesized by Bacon lie above this curve.

As filament diameter increases, the probability increases that voids and defects will arise during char formation. This is particularly true since gaseous products stand less chance of escaping from the interior of a large mass. On the other hand, voids and defects, while probable, can be more easily controlled in pyrolytic deposits.

II. LARGE DIAMETER CARBON MONOFILAMENT DEVELOPMENT

A. CHEMICAL VAPOR DEPOSITION

The formation of continuous filaments by chemical vapor deposition generally involves the conversion of a thermally decomposable gas into the desired filamentary material on a heated substrate. The heated substrate generates the necessary energy required for chemical conversion of the gas to a solid and, in addition, provides a site for nucleation and growth of the deposit. Under controlled conditions, the deposit is built up layer by layer to provide a relatively non-porous material.

B. ADVANTAGES OF CVD PROCESS

In view of the problems of voids and defects inherent in pyrolytic processes and the long diffusion times required to evolve volatiles, etc., Hough Laboratory chose the CVD method to make large diameter monofilaments for the following reasons:

1. Low porosity materials can be synthesized;
2. Composition of the deposit can be controllably varied;
3. High purity deposits are possible; and
4. Degree of crystallinity and crystal order can be controlled.

The successful and reproducible synthesis of large diameter graphite monofilament having a high-strength, high-modulus is contingent upon the attainment of a suitable compromise between the demonstrated very high strength,

very high modulus properties of perfect three-dimensional ordered sublimed graphite and the basal plane slippage reduction inherent in a less ordered material. Graphitizable carbon derived by pyrolysis of organic precursors has demonstrated this compromise in small diameter fibers (point E, Figure 1). However, suitable time-temperature processing parameters have now been realized for synthesis of large diameter fibers by this route. Catastrophic disintegration as volatiles are released may be a limiting factor.

On the other hand, larger diameter pyrolytic graphite whiskers have been synthesized with reasonably high strengths (points C and D, Figure 1). Here, order/disorder effects are evidently compromised. The vapor deposition process for the synthesis of pyrolytic graphite involves a build-up layer by layer from the gaseous state. This method, therefore, offers the potential for controlling the order/disorder of the carbon. For example, microstructural effects have been observed when soot is added to the plating atmosphere or when gas phase nucleation of soot is permitted during the formation of bulk pyrolytic graphite. The resulting structure appears as a continuously nucleated system of small growth cones. Stover (Reference 14) identifies the origin of these cones with tiny conical whiskers growing spirally with the deposit.

Methods for achieving basal plane locking might include: (1) whiskers growing normal to the basal planes; (2) a somewhat random crystallite orientation; or (3) the utilization of carbon-based alloys.

III. PROCESS

A. EQUIPMENT

The processing equipment utilized in this developmental program is essentially a long cylinder through which the substrate material is drawn by means of a motor driven take-up spool. A simple braking device on the supply spool provides proper substrate tension. The ends are sealed by capillaries which allow passage of the substrate into the cylinder and passage of the synthesized fiber out from the cylinder. For vacuum deposition conditions, end seals functionally similar to those first reported by Moers (Reference 15) are employed.

The chemical vapor deposition reaction is initiated by the "hot wire" method wherein the substrate is drawn across two or more electrodes and heated resistively to the required deposition temperature. A typical electrode configuration is diagramed in Figure 3.

The ion bombardment experiments were performed by inserting additional electrode elements (two-stages) into the plating atmosphere and establishing an electrical discharge between the electrode element and the moving fiber in a direction normal to the fiber surface.

B. SUBSTRATE

Carbon monofilament was chosen over other materials such as tungsten fine wire. Factors included in this choice were:

1. strength at the required deposition temperatures;
2. availability in diameters of nominal 1.0 to 1.3 mils (25 to 33 μ);
3. capacity to be resistance-heated;
4. no reaction with the pyrolytic deposit; and
5. very smooth surface which reduces irregularities in the deposit.

C. PLATING ATMOSPHERE

Virtually any gaseous hydrocarbon will decompose at sufficiently high temperatures, yielding pyrolytic carbon. A number of precursor hydrocarbons with and without various functional groups have been examined (Reference 10). The utilization of additives, as alkyl iodides, to act as free radical sinks to prevent soot formation and yield finer structured pyrolytic carbon deposits is known (Reference 16).

We did not find any plating atmosphere which would yield pyrolytic graphite fibers of significantly high strength even with the addition of free radical sinks. We did find that the addition of alloying elements to the plating atmosphere produced marked improvement in fiber strength. Of additives tried, such as boron, silicon and aluminum, the most significant improvement was produced by boron.

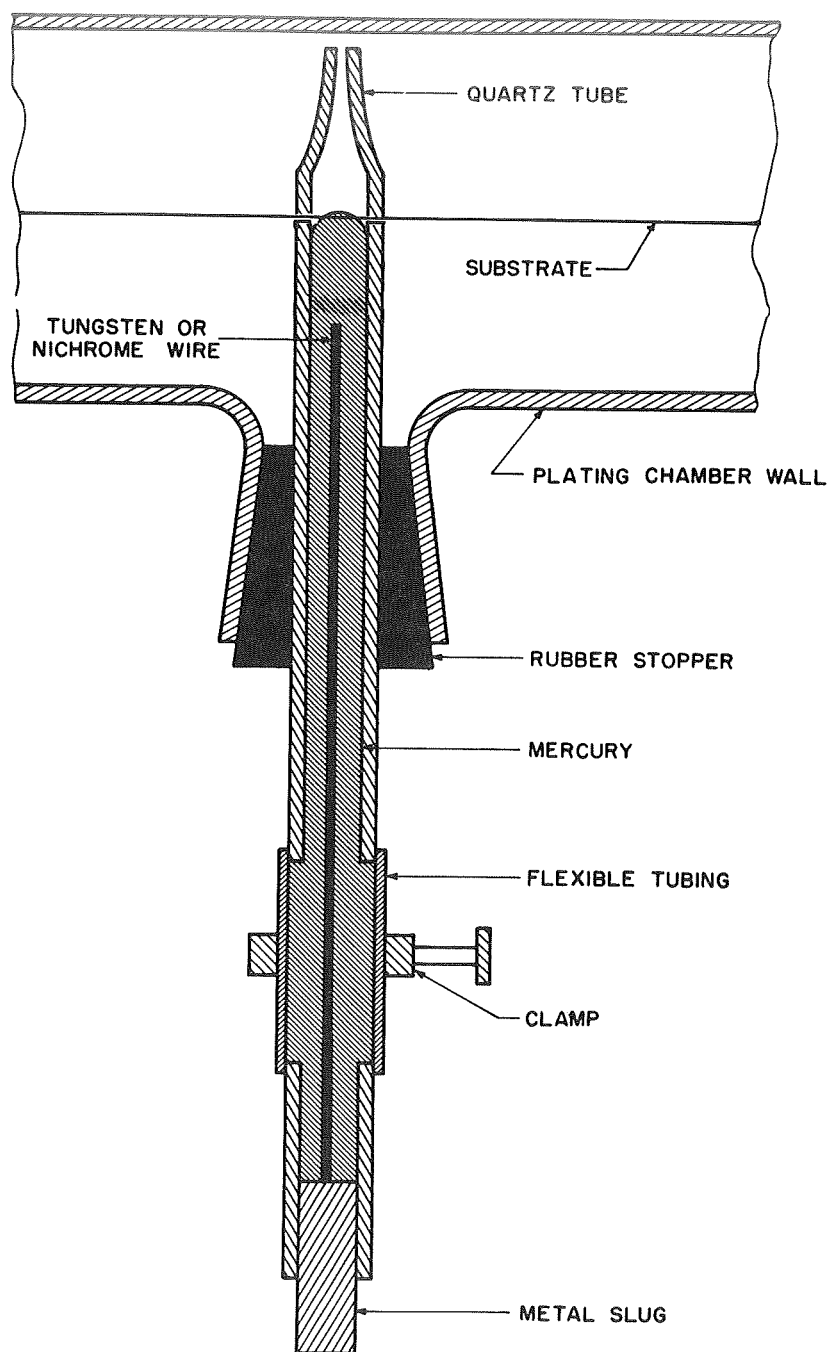


Figure 3 - Typical Electrode Configuration

IV. FIBER CHARACTERIZATION

A. ULTIMATE TENSILE STRENGTH

This property is determined by conventional load cell methods utilizing either a two or ten pound load cell coupled to a Statham transducer. Loading rate is 0.05 in/min. (0.127 cm/min.) on a 0.25 in. (0.64 cm) length.

B. MODULUS

The modulus is determined by the "vibrating reed" technique (Reference 17 and 18). This method was used by Elkins, Mallan and Shimizu (Reference 19) to determine modulus for experimental silicon carbide continuous filaments. More recently, Alexander, et al, have reported the use of this method (Reference 20).

A length of the sample fiber (1.0 inch \pm 0.01 inch or 2.54 cm \pm 0.03 cm) is affixed at one end to a magnetic transducer driven by the amplified sine wave from an audio-frequency generator. The generator is calibrated by the Lissajous Figure method. The frequency is recorded at which maximum vibration occurs for the free end of the fiber.

The modulus is determined from the relationship:

$$M = \frac{f^2 l^4 \rho}{7.58 d^2}$$

where l = length (in.)

M = elastic modulus (psi)

f = resonant frequency (Hertz)

ρ = density (lb/in³)

d = fiber diameter (inches)

Using this method, boron filament was found to have a modulus of 58×10^6 psi (40×10^6 N/cm²) which is in agreement with accepted range of values.

C. DENSITY

Density is determined by the floatation method in which two liquids (tetrabromoethane and dichloroethane) are mixed in such proportions that a

short section of fiber placed beneath the surface of the liquids remains suspended therein. Density is also checked by actually weighing a nominal 10 foot (3.048 meters) length of filament and determining volume on the assumption that fiber diameter is invariant for the specimen.

D. HIGH TEMPERATURE TENSILE STRENGTH

We determined that heat treatment for 24 hours at 1472°F (800°C) in argon does not weaken the fibers. Accordingly, we performed a limited effort to tensile test the fiber at temperatures to 1832°F (1000°C). A small furnace was designed which fits directly on the tensile testing machine. Direct resistance heating of the filament is achieved by mercury standpipe electrodes spaced 0.6 inches (1.53 cm) apart. A window is provided for temperature measurement by optical pyrometry.

Before improving our testing procedure, the technical effort was re-directed toward fiber improvement.

E. STRUCTURE

X-ray diffraction studies have been performed on both highest strength graphite fiber and the boron-carbon alloy.

A Jarrell-Ash Microfocus unit and Jarrell-Ash camera were used. The sample was mounted in the camera and rotated while being exposed to nickel filtered copper K_{α} radiation. Exposure periods ranged from 30 minutes to one hour.

F. COMPOSITION

Elemental analysis of the fibers with respect to boron content was performed by Galbraith Laboratory, Knoxville, Tennessee. The addition of this element to the carbon improved the fiber strength. A range of nominal 25 to 35 weight per cent boron was used in this program. No systematic attempt was made to correlate fiber properties with respect to boron content.

V. RESULTS AND DISCUSSION

A. TUNGSTEN SUBSTRATE

Our initial efforts under this program concerned the formation of continuous pyrolytic graphite on 0.5 mil (12μ) and 1.0 mil (25μ) diameter tungsten substrates and synthesized at a temperature of 2000°C to 2400°C . Uneven growths (Figure 4), arising from preferred nucleation along die imperfection marks in the drawn tungsten wire, are believed to have limited the measurable strength level. Gas phase nucleation of soots, which form inclusions in the deposit, also produce weak fibers. The utilization of vacuum deposition conditions and the addition of free radical "sinks" as iodides to the plating atmosphere reduced these effects, thus yielding smoother surfaced filaments (Figure 5). At best, U. T. S. values of ca. 80,000 psi ($44,120\text{ N/cm}^2$) and modulus of ca. 15,000,000 - 18,000,000 psi ($10,335,000 - 12,402,000\text{ N/cm}^2$) were found for fibers of nominal 3.0 - 4.0 mils ($75 - 100\mu$) diameter (point D, Figure 2).

It is the opinion of the author that the free radical sinks mentioned above function in reducing uneven pyrolytic growth by combining with hydrocarbon containing free radicals, thus preventing them from agglomerating and reaching a critical aggregate size in the chemical vapor deposition atmosphere. In the case of the thermal gradient existent near the hot tungsten wire substrate, the absence of these aggregates precludes extensive gas phase nucleation and growth of pyrolytic soots and allows the super-saturated gas to condense without extensive soot inclusions and form a relatively smooth deposit on the wire substrate.

B. CARBON SUBSTRATE

Because of the problems encountered using the tungsten substrate, we decided to shift emphasis to a carbon substrate. The use of a smooth carbon substrate results in elimination of uneven growth structures that might otherwise arise from substrate topographical anomalies (Figure 6). Highest

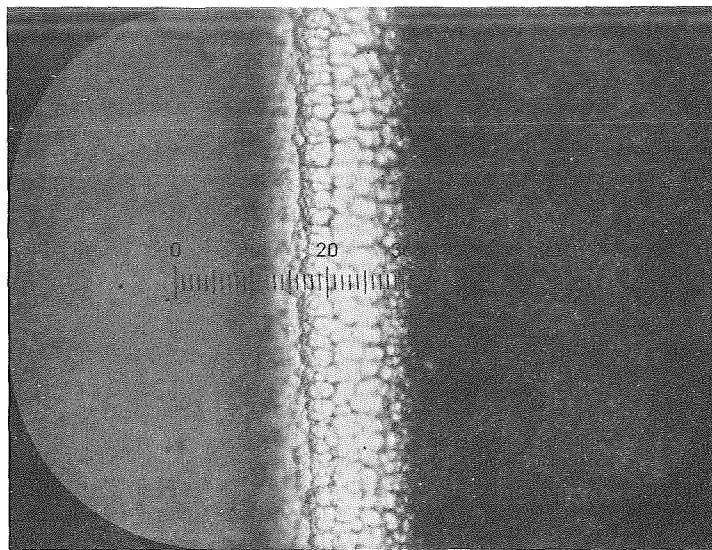


Figure 4 - Uneven Pyrolytic Graphite Growth Along Tungsten Substrate Ridges

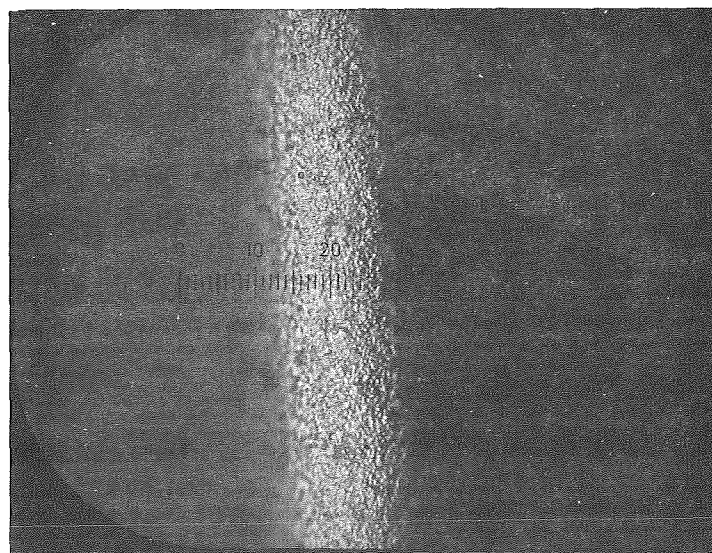


Figure 5 - Smoother Pyrolytic Graphite Growth on Tungsten

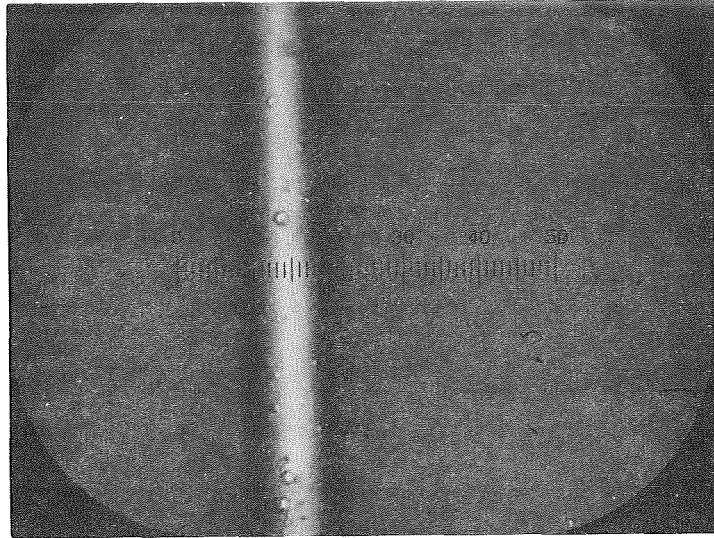


Figure 6 - 1.5 mil (37 μ) Smooth-Surfaced
Pyrolytic Graphite Fiber on Carbon

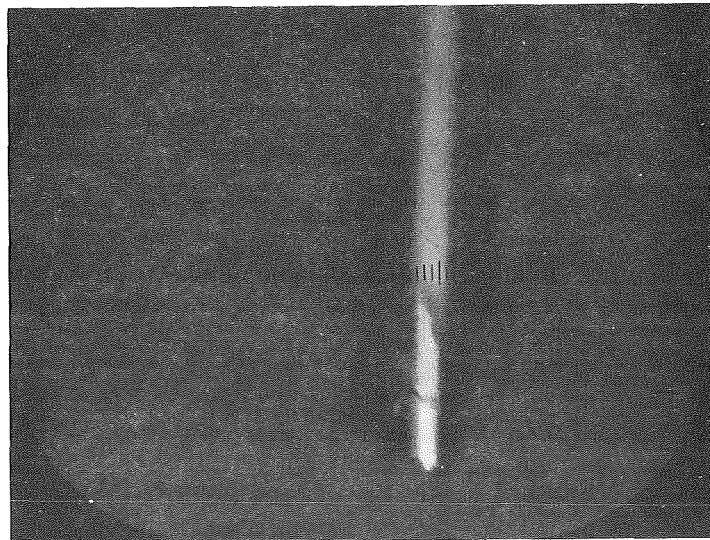


Figure 7 - Telescope Fracture in Tension

strength/modulus values obtained for carbon substrate pyrolytic graphite fibers are nominally 160,000 psi ($110,240 \text{ N/cm}^2$) and 18,000,000 psi ($12,402,000 \text{ N/cm}^2$) respectively at a diameter of nominal 1.5 mils (37μ) (see point E, Figure 2). These were synthesized at 1100° to 1400°C . Thus, Figure 7 displays a typical telescopic fracture at 65,000 psi ($44,785 \text{ N/cm}^2$) observed for a 1.9 mil (48.5μ) diameter fiber having a 1.0 mil (25μ) diameter carbon core and synthesized at ca. 2000°C . Figure 8 shows in cross-section a pyrolytic graphite fiber of nominal 3.0 mil (76μ) diameter. Internal delamination rings are evident for these large diameter fibers. Basal plane slippage and delamination are apparent strength limiting mechanisms for these fibers irrespective of synthesis temperature.

The weakening effects of delamination and plane slippage might be reduced by basal plane locking in the form of radially deployed whiskers within the pyrolytic graphite structure or by introducing various "alloying" agents. Experiments utilizing two-stage ion bombardment methods to deploy whisker-like structures were performed. Two-stages were utilized to nucleate and then grow the whiskers and matrix. No significant increase in strength was obtained. The resulting fibers were somewhat rough and the substrate was not centrally located within the fiber. Preferential fiber growth was in the direction of the ion stream (white arrow in Figure 9).

The addition of alloying agents to the plating atmosphere during the ion bombardment experiments suggests that a thorough examination of the alloying of carbon with boron will produce marked strengthening effects. Attempts were made to synthesize carbon alloy fibers containing aluminum or silicon by the "hot wire" method. These fibers were found to have rough uneven surfaces and were so brittle that we did not attempt to determine strength. Utilizing the "hot wire" method, carbon alloy fibers were synthesized having a maximum experimental strength/modulus of 465,000 psi ($320,385 \text{ N/cm}^2$) and 28,000,000 psi ($19,292,000 \text{ N/cm}^2$) respectively. The plating atmosphere contained hydrogen, argon, ethylene, and triethyl borane. The point F in Figure 2 represents this maximum for a filament 3.57 mils (90μ) diameter. These carbon alloy fibers have relatively smooth surfaces (Figure 10), though some surface defects are observable. Thus, Figures 11a and 11b represent a U. T. S. fracture which initiated at a nodular growth on the filament

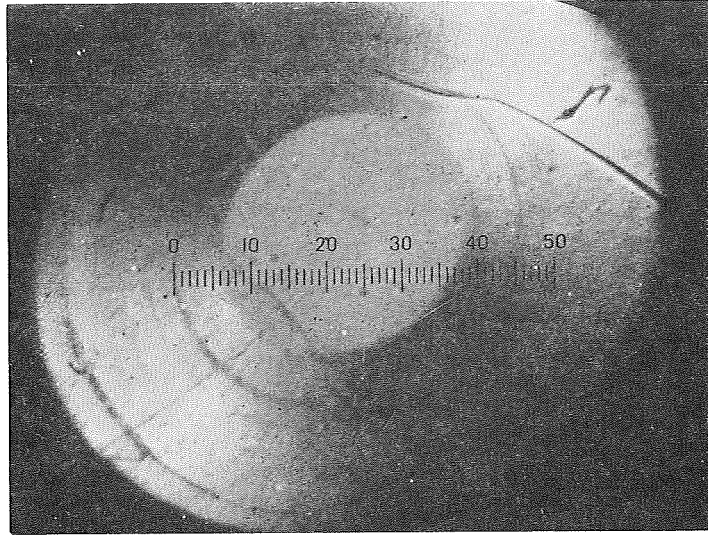


Figure 8 - Cross-Section - Delaminated Pyrolytic Graphite on Carbon

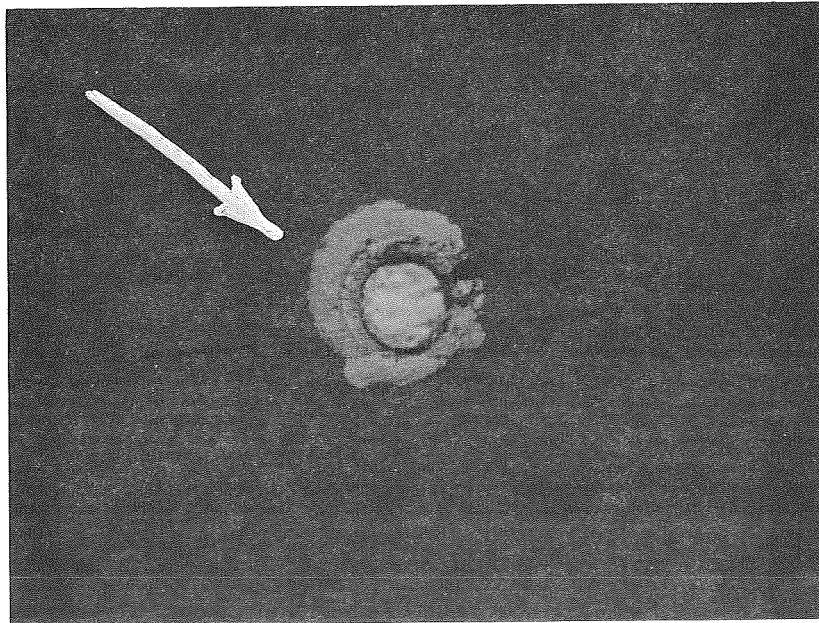


Figure 9 - Carbon Deposit by Ion Bombardment

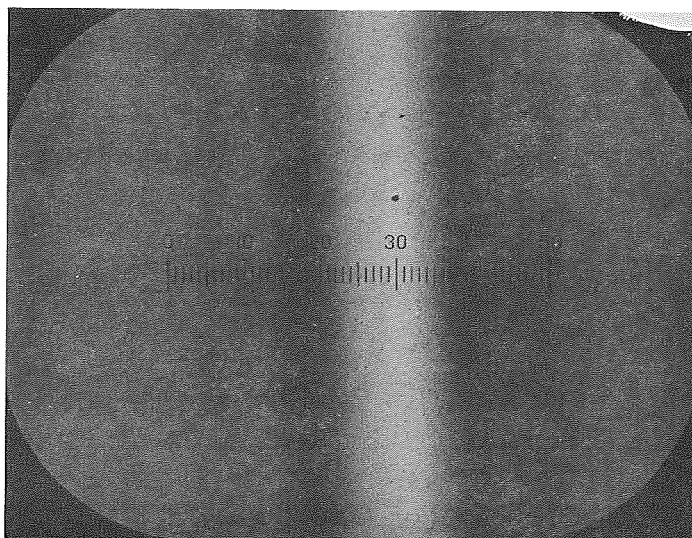


Figure 10 - Carbon-Alloy Fiber Surface

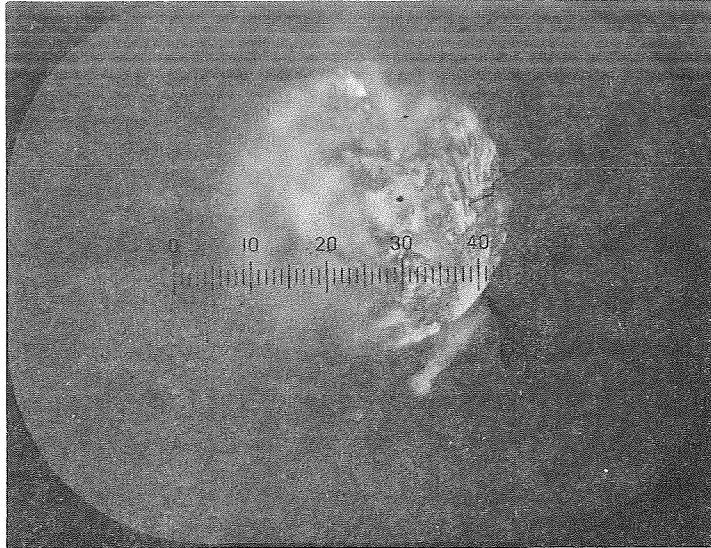


Figure 11a

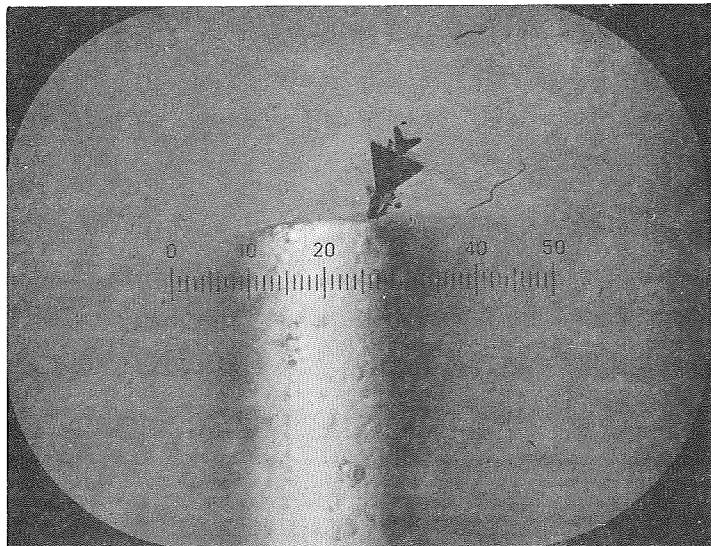


Figure 11b

Fracture Initiated at a Nodule

surface. These defects appear to limit current production fibers to a nominal 300,000 psi (207,000 N/cm²) ultimate tensile strength. Such defects may arise from:

1. Gas-borne particles of dirt;
2. Dirt particles from the electrode contacts;
3. Gas-phase nucleation of soots; and/or
4. Insulative oils, tars, etc., which may condense on the cooler portions of the filament, causing downstream electrode arcing.

These high strength fibers exhibit glassy fractures in bending (Figure 12). Fractures observed in tensile loading above 400,000 psi (275,000 N/cm²) show features exemplified by the SEM views of Figures 13a and 13b.

Evidently the effect of alloying boron into the carbon is to reduce the formation of large crystallites and stabilize the carbon as a very fine grained essentially amorphous substance. In this form many pyrolytic materials, as for example boron, exhibit high strength. The relative strength of the respective components of these fibers, namely the boron and the carbon, are not known. The modulus is approximately twice that of unalloyed pyrolytic graphite fibers. Further research is required to determine the optimum boron content.

The carbon alloy appears to exist as a very fine grained matrix containing nominally 25 - 30% highly orientated tetragonal boron. The boron content was determined by chemical analysis and by X-ray diffraction.

Maximum strength/diameter vs. month for the monofilament development is displayed in Figure 14. The alloy fibers have a density of ca. 0.0688 lb./cu.in. (1.91 g/cc). This corresponds to a maximum specific strength of 6.8 x 10⁶ in. (17.2 x 10⁶ cm.) and a specific modulus of 403 x 10⁶ in. (10.2 x 10⁸ cm.).

C. PROCESSING PROBLEM AREAS

Our present thinking is that the ultimate tensile strength is a function of variables such that

$$S = f \left[I, v, \phi_1, \phi_2, \frac{\partial \phi_T}{\partial t} \right]$$

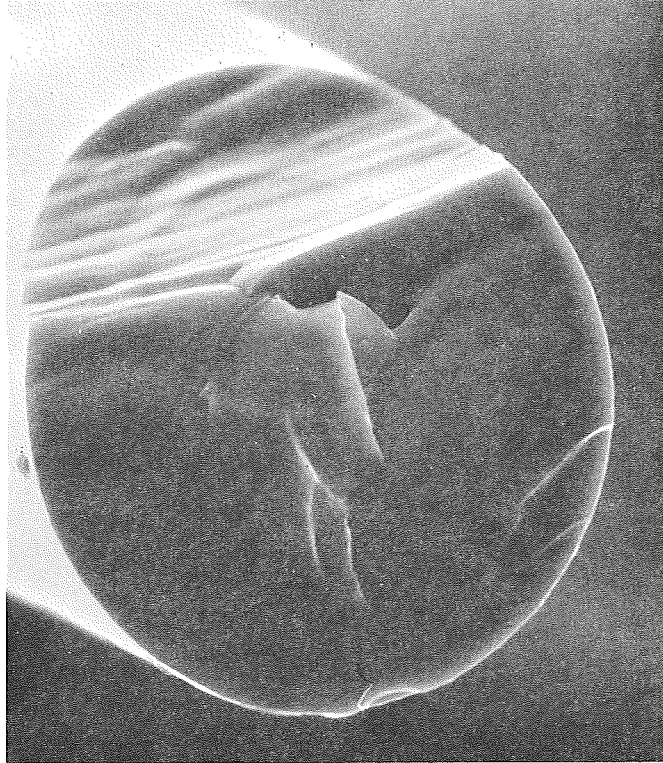


Figure 12 - SEM View of Carbon-Alloy Fracture in Bending

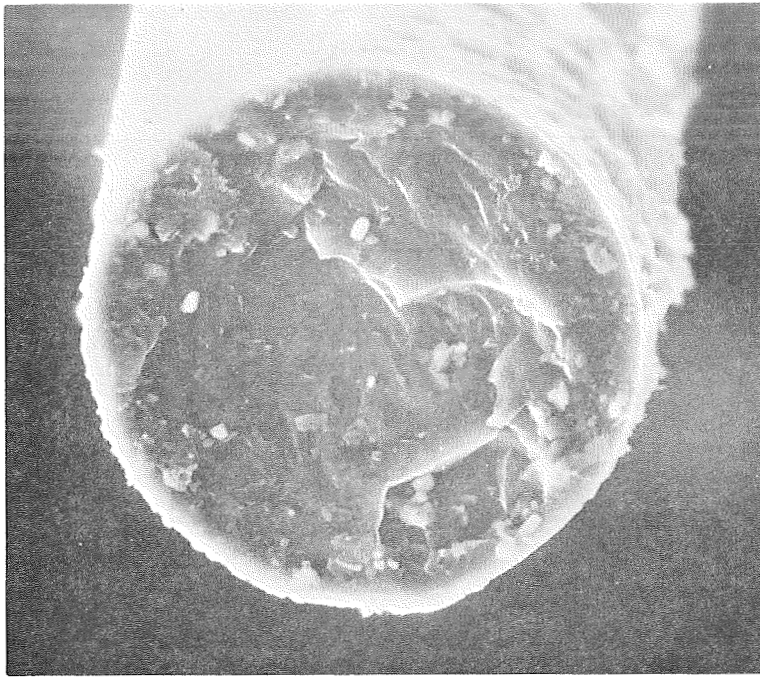


Figure 13a - SEM View of Carbon-Alloy Tensile Fracture
> 400,000 psi (276,000 N/cm²)

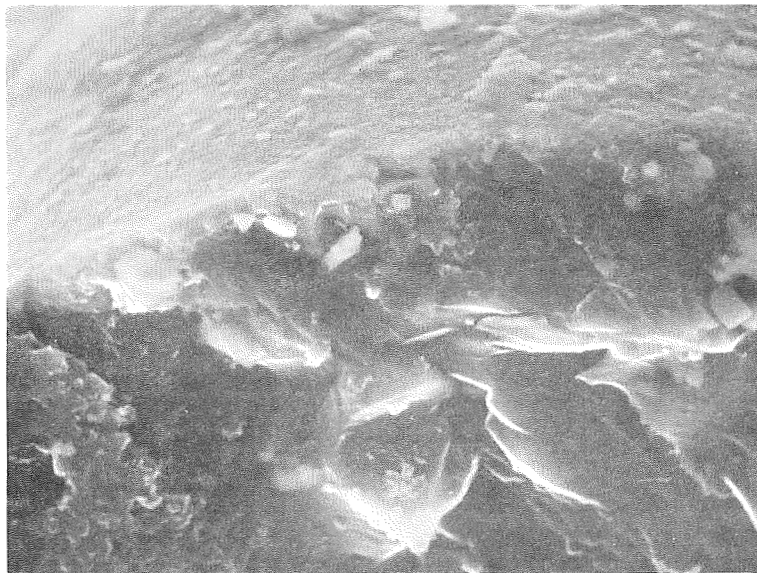


Figure 13b - Close-up SEM View of Figure 12a

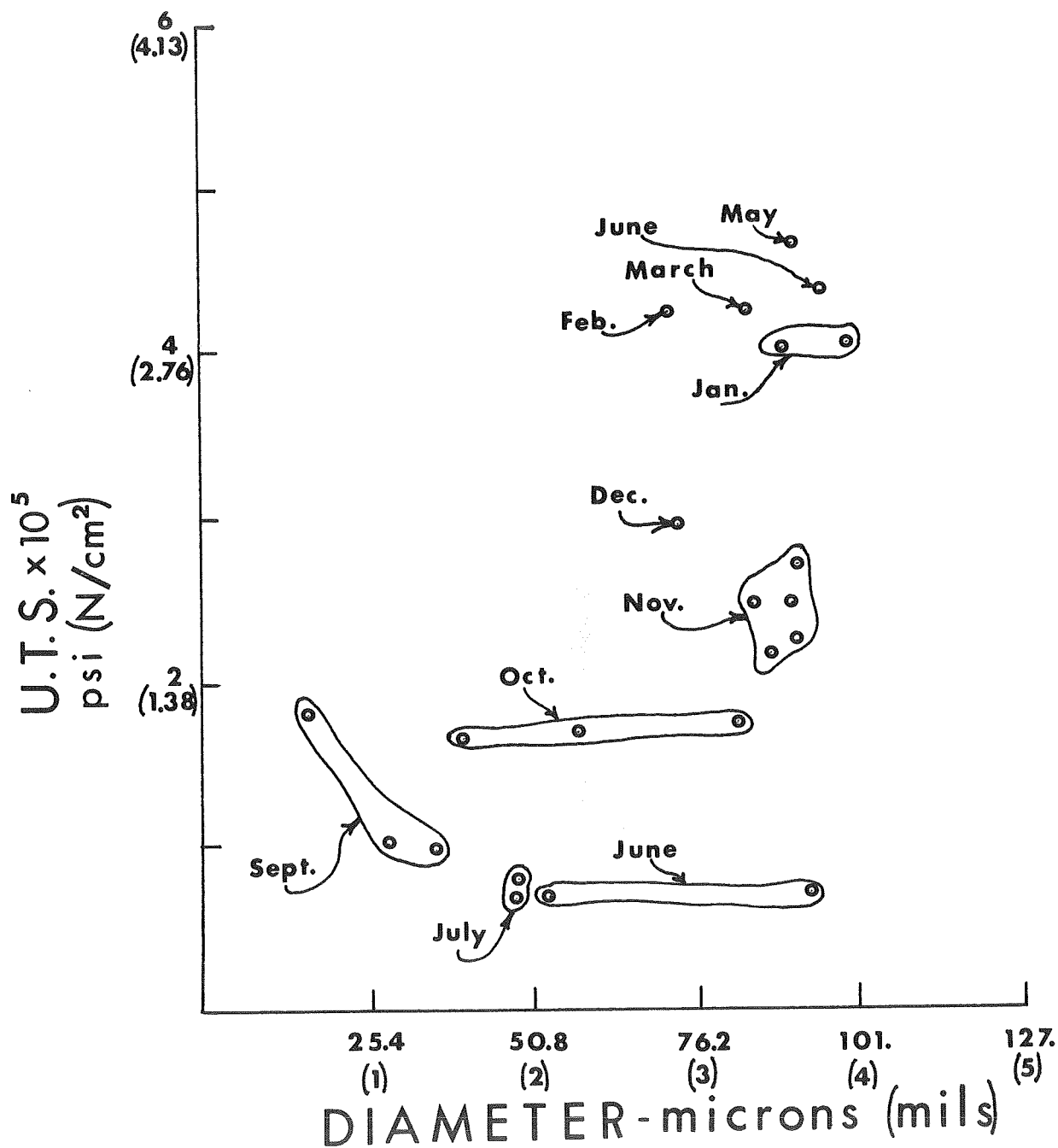


Figure 14 - Strength-Diameter vs. Month for Monofilament Development

where S = ultimate tensile strength
 I = heating current
 v = fiber synthesis velocity
 Φ_1 = ratio of boron to carbon in the plating gas
 Φ_2 = mole % carbon in plating gas
 $\frac{\partial \Phi_T}{\partial t}$ = total gas flow rate

Consider now Figure 15. Figure 15 represents the first octant defined by I , v , and Φ_1 . The nested surfaces A_n , B_n , C_n are contained in the first octant and represent various values for S such that

$$S_A < S_B < S_C$$

The values $n = 1$, $n = 2$, $n = 3$ represent possible displacements affected by fixed values for either Φ_2 and/or $\partial \Phi_T / \partial t$.

We believe that the closed surface representation is permissible since our experimental findings to date suggest that there does indeed exist a spherical neighborhood about some point in octant I such that all values for a given S are contained therein.

Obtaining reproducible high strengths has been a problem. The prime difficulty is believed to be variations in the synthesis variables mentioned above. Thus, the variations may cause us to drift into a region of high strength filament synthesis parameters only to drift into a lower region, even during a single synthesis run.

One variable, velocity, is known to have varied. We noted a gradual change in motor speed with respect to time for the D. C. feed-back controlled system. Previously, we found that low motor speeds produce insufficient feed-back signals such that generator brush contact variations induce erroneous controller output. By going to higher gear reduction ratios, we reduced this problem to what was considered an acceptable level. However, we then noted the possibility that thermal variations in the control circuit itself could give further velocity drifting. By installing synchronous motor drives having fixed shaft speeds, we eliminated synthesis velocity drift.

Another variable which experienced drifting is heating current. Previously, we have been manually adjusting this variable to maintain a constant

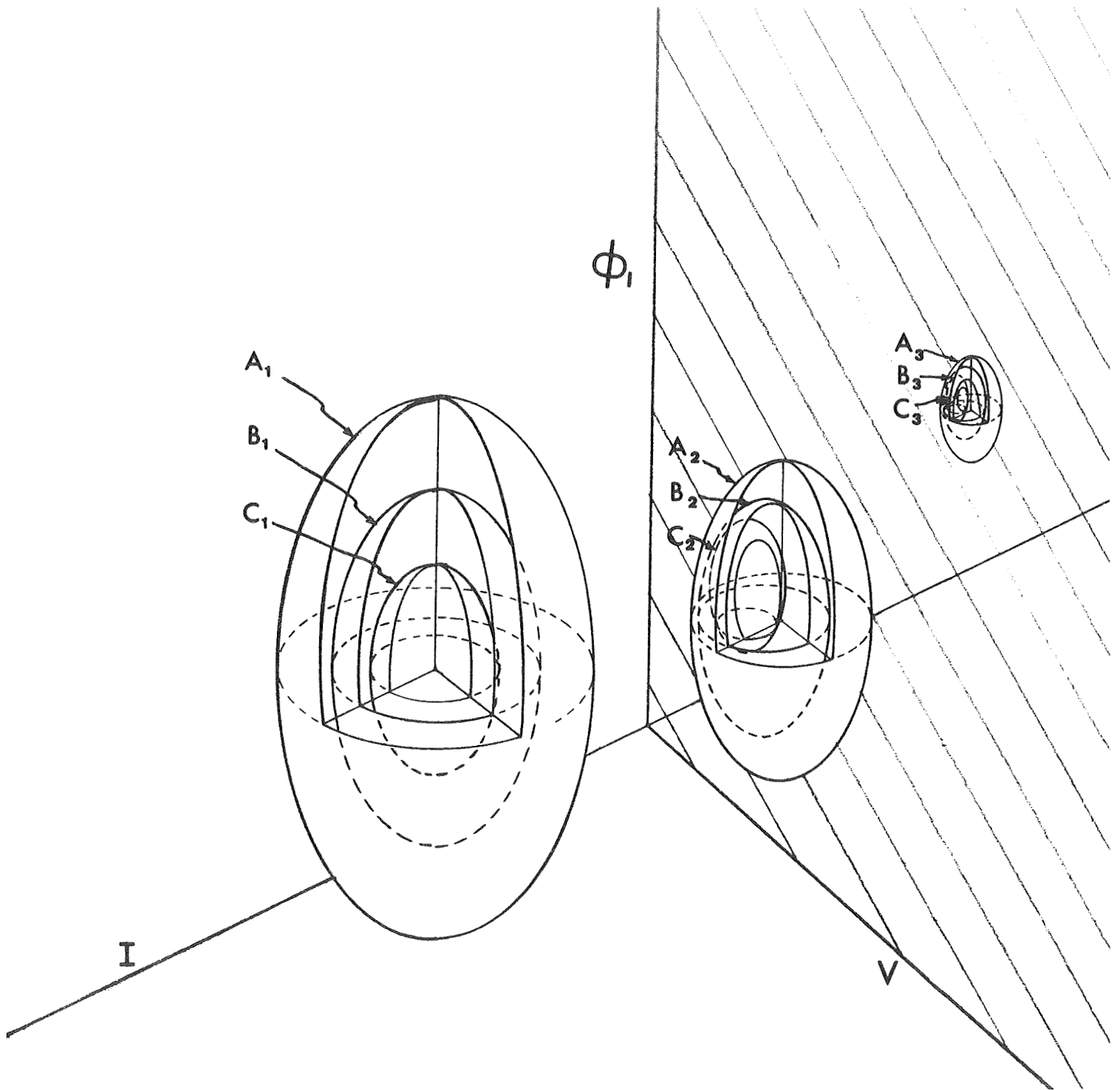


Figure 15 - Proposed Functional Relationship of Process Variables

value. We have now checked out a saturable reactance control driven by a triac circuit. The triac receives a variable signal from a photoresistive element mounted inside an indicating meter which monitors the CVD cell.

The ratio of boron to carbon appears to be such that a nominal 25 to 35 mole per cent boron in carbon offers best fiber strength.

The total mole concentration of carbon in the plating atmosphere is closely associated with total gas flow rate. These variables have not been sufficiently investigated to determine optimum plating conditions.

D. FIBER DEFECTS

The presence of defects in the fibers is evident in the measured strength of current production fibers. Experimental fiber strengths have reached measured values to 541,000 psi ($372,000 \text{ N/cm}^2$) for a 3.57 mil (90.8μ) fiber. We believe that we are currently limited to production runs yielding fibers of nominal 300,000 psi ($207,000 \text{ N/cm}^2$). Such defects may arise from dirt inclusions derived from such sources as:

1. Gas-borne particles;
2. Electrode contacts;
3. Gas-phase nucleation of soots; and/or
4. Insulative oils, tars, etc.

1. Gas-Borne Dirt Particles

We installed molecular sieve driers and micropore filters in all gas lines. A reduction in population density of particle induced aggregate was noted for the synthesized filament. This gas-borne dirt may arise from rust, oils, etc., existent in compressed gas cylinders themselves.

2. Dirt from Electrodes

Because of the special design of the electrodes used in this study, we do not believe that defects are arising from this source.

3. Gas-Phase Nucleation of Soots

A series of experiments conducted during February 1970 was designed to specifically alter the gas flow pattern in the plating cell. The alterations changed the flow pattern mainly in the upstream portion of the cell.

We found a very pronounced correlation between gas flow and the nodule density. For example, a very restricted flow of gas at the electrodes caused an increase in nodules. Soots are caused by premature thermal decomposition, nucleation and growth of solids in the plating atmosphere. We believe that this gas-phase nucleation of soots which then migrate to the growing pyrolytic surface is the main source for inclusion-induced nodular defects.

4. Insulative Tars, Oils, Etc.

Defects arising from this source have not been observed.

E. CRYSTALLOGRAPHIC STRUCTURE

The crystallographic structure of the fibers synthesized under this program was studied utilizing a Jarrell-Ash microfocusing unit with a Jarrell-Ash camera. Copper K_{α} radiation with nickel filtering was utilized with the fiber sample rotated in the X-ray beam for periods of 30 minutes to one hour. For the graphite material, we find that the graphitic basal planes are preferentially orientated with the c-axis perpendicular to the fiber axis. An estimated 90 to 95% c-axis orientation is within 22° of normal. When we examine the boron-carbon alloy, we find an apparent reduction in X-ray diffraction ring sharpness for higher strength fibers. This suggests that a more amorphous structure results in higher strengths.

X-ray diffraction using the Cu K nickel filtered radiation displays three rings for the carbon-boron alloy fiber. Thus:

θ	$d(\text{\AA})$	(carbon)— $\frac{hkl}{\text{hk1}}$ —(tetragonal boron)
13.15	3.390	002 300
21.25	2.127	100
27.10	1.692	004

The 3.390 Å ring shows an (amorphous) graphite ring with a sharp, highly orientated overlying ring corresponding with the 300 plane of tetragonal boron (see Figure 16). The overlying ring amounts to, perhaps, 20 - 25% of the total energy. As stated above, a broadening of these rings is attended by an apparent increase in fiber strength.

The above mentioned structure is reminiscent of the work of Hammond, Lindquist and Bragg (Reference 21) on boron filaments. They report that the boron is composed primarily of 10 to 100 Å crystallites of α -rhombohedral boron and possibly some tetragonal boron. Inclusions of both α - and β -rhombohedral boron, 100 to 10,000 Å in diameter were found scattered throughout the boron matrix. They observed that the X-ray halo pattern is best interpreted as a mixture of the α -rhombohedral and "simple" tetragonal polymorphs. They further noted that observed density fits closely to a mixture of 74% α -rhombohedral boron, 24% tetragonal boron and 2% porosity.

F. COMPARISON OF PROPERTIES

The properties of the monofilaments developed in this program, when compared with competitive filaments, are attractive. Generally these fibers have:

1. Superior strengths;
2. Competitive modulus;
3. Low density;
4. Larger diameters than available carbon fibers; and
5. High specific strength and competitive specific modulus because of low density.

The unique position occupied by these experimental fibers based upon specific strength (U. T. S./density) is displayed in Figure 17. We note that, of the 23 materials displayed, only Thornel 100 (experimental) has a higher specific strength.

While the current specific modulus value for these fibers is not high, it is at least competitive compared to other materials as shown in Figure 18.

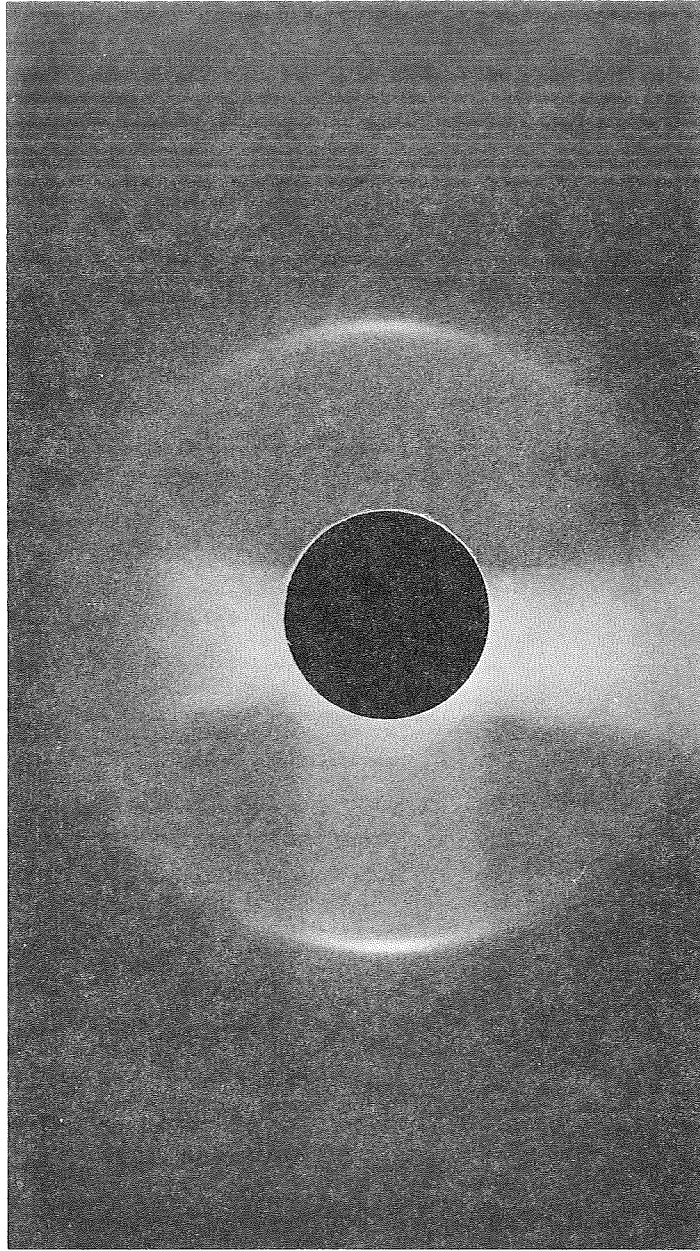


Figure 16 - X-ray Diffraction Pattern for Carbon-Alloy Fiber

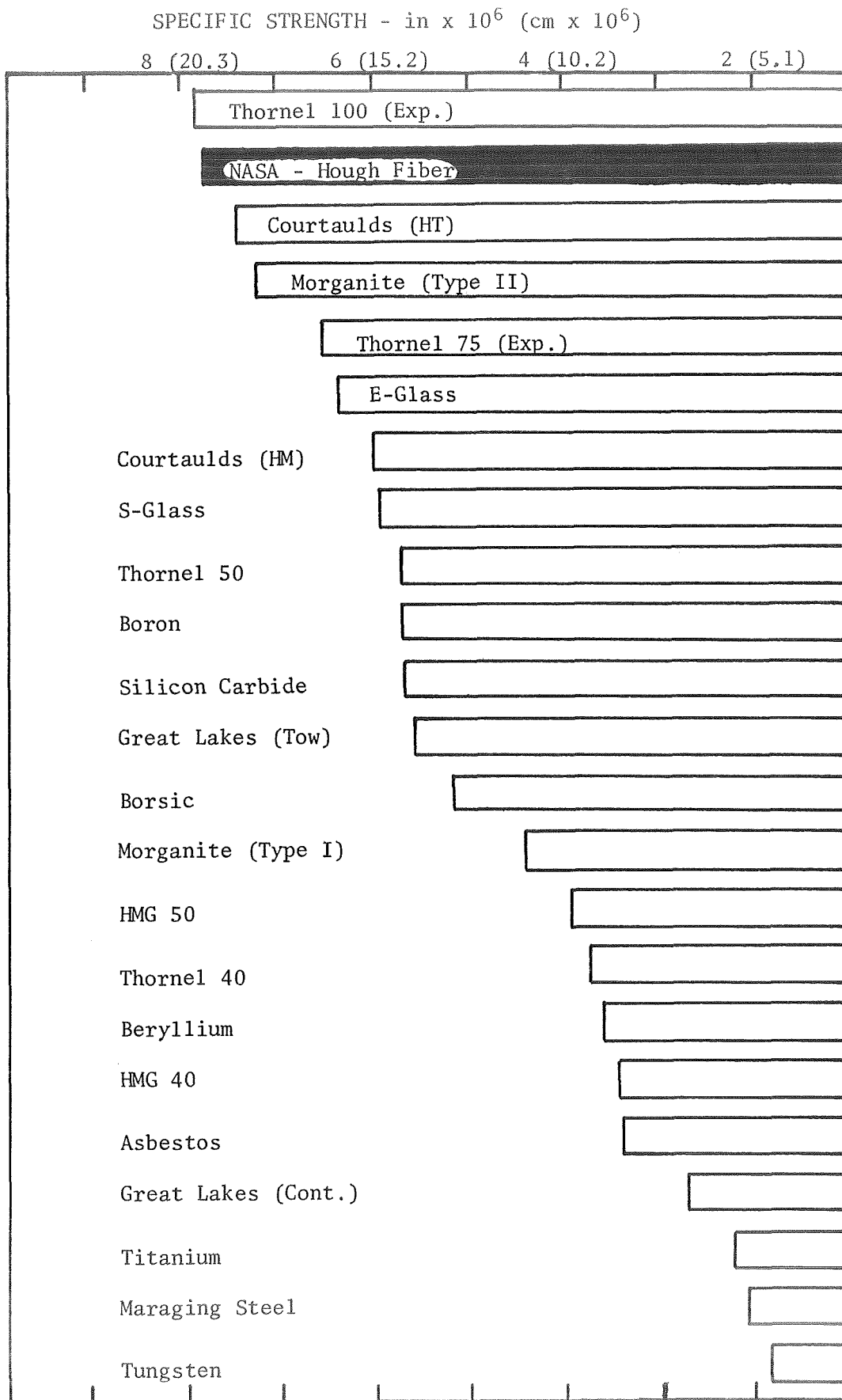


Figure 17 - Specific Strength vs. Selected Filaments

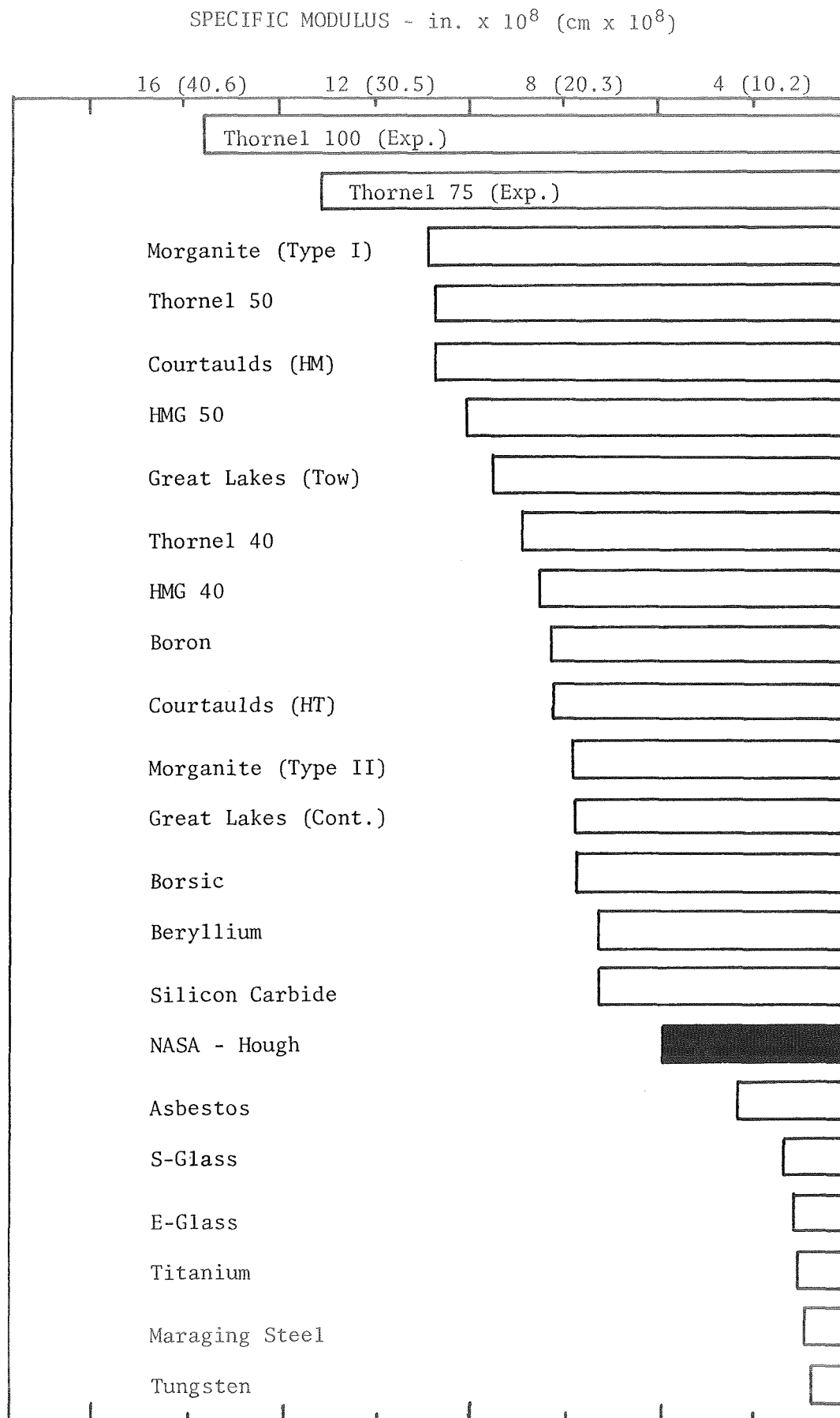


Figure 18 - Specific Modulus vs. Selected Filaments

VI. CONCLUSIONS

Conclusions reached during this program are:

1. The CVD method has shown dramatic strength increases. A dramatic strength increase is observed when boron is alloyed with the pyrolytic carbon. Experimental U. T. S. values up to 541,000 psi ($372,000 \text{ N/cm}^2$) and an elastic modulus of 27.7×10^6 psi ($19.1 \times 10^6 \text{ N/cm}^2$) have been measured on fibers of nominal 3.57 mils (90.6μ) diameter. These properties are superior to those of other forms of carbon fibers.

2. The boron appears to exist as a highly orientated tetragonal phase in an amorphous carbon matrix. Currently it is believed that ca. 25 to 35 mole per cent boron in carbon is the preferred concentration level for this alloy.

3. Carbon substrates do not appear to react with the chemical vapor deposited material. In this respect, carbon is preferred over tungsten fine wires which do react and, therefore, disrupt the early nucleation and growth phases of the synthesis of large diameter carbon or carbon-alloy fibers.

4. Pyrolytic carbon fibers synthesized at temperatures of 3632°F (2000°C) fracture in tension predominantly in a telescopic mode. This appears to be caused by delamination of the graphitic basal planes as the fibers cool from synthesis temperature. The phenomenon is observed to occur at loadings of ca. 65,000 psi ($41,300 \text{ N/cm}^2$) for fibers having diameters on the 2.0 mil (51μ) to 4.0 mil (102μ) range.

5. Pyrolytic carbon fibers synthesized at lower temperatures (2012°F - 2552°F , 1100°C - 1400°C) contain fewer delaminations but are still limited to strength levels of ca. 150,000 psi ($103,000 \text{ N/cm}^2$) in the nominal 2.0 mil (51μ) to 4.0 mil (102μ) diameter range.

6. Fiber strength is believed to be limited by defects in the filament structure caused by gas phase nucleated soots which become trapped within the growing deposit.

7. Additional research is necessary to upgrade the filament and to increase production rate which is currently limited to 0.75 fpm (0.228 meters per minute).

REFERENCES

1. R. Bacon, "Growth, Structure, and Properties of Graphite Whiskers," J. Appl. Phys. 31.2, February 1960, pp. 283 - 290.
2. R. Bourdeau, private communication, August 1964.
3. F. E. Papalegis and R. G. Bourdeau, "Pyrolytic Reinforcing Agents for Ablative Erosion-Resistant Composites," ASD-TDR-63-403, May 1963, W-PAFB, Ohio.
4. F. E. Papalegis and R. G. Bourdeau, "Pyrolytic Reinforcements for Ablative Plastic Composites," ML-TDR-64-201, July 1964, W-PAFB, Ohio.
5. R. G. Bourdeau, private communication, August 1969.
6. R. Bacon, "High Strength - High Modulus Carbon Fibers," AFML-TR-66-334, Part I, December 1966, W-PAFB, Ohio.
7. S. Otani, "On the Carbon Fiber from the Molten Pyrolysis Products," Carbon 3, Pergamon Press Ltd., Great Britain, 1965, pp. 31 - 38.
8. W. R. Benn, private communication, June 1969.
9. E. R. Stover and R. R. Berning, "Effects of Strain-Annealing on Structure and Mechanical Properties of Pyrolytic Graphite," Paper No. 111, Fifth Biennial Conference on Carbon, The American Carbon Committee, University Park, Pennsylvania, June 19 - 23, 1961.
10. R. L. Hough, "Continuous Pyrolytic Graphite Filaments," AFML-TR-64-336, December 1964, W-PAFB, Ohio.
11. R. L. Hough, "Continuous Pyrolytic Graphite Composite Filaments," J.AIAA 3.2, February 1965, pp. 291 - 296.
12. R. H. Clinard, Texaco Experiment Inc., private communication, October 1967.
13. R. H. Clinard, Texaco Experiment Inc., private communication, September 1969.
14. E. R. Stover, General Electric Company Report 64-RL-3609M, March 1964.
15. K. Moers, German Patent 567,955, December 22, 1932.
16. R. L. Hough, U. S. Patent 3,379,555, April 23, 1968.

17. A. S. Nowich, Resonance and Relaxation in Metals, 2nd Edition, Plenum Press, New York, 1964.
18. P. M. Morse, Vibration and Sound, McGraw-Hill Book Company, Inc., New York, 1948.
19. P. E. Elkins, G. M. Mallam and H. Shimizu, "Modified Silicon-Carbide Continuous Filaments," Paper D-41, SAMPE, Vol. 10, 10th National Symposium and Exhibit, San Diego, Calif., Nov. 9 - 11, 1966.
20. J. A. Alexander, A. L. Cunningham and K. C. Chuang, "Investigation to Produce Metal Matrix Composites with High-Modulus, Low-Density Continuous-Filament Reinforcements," AFML-TR-67-391, W-PAFB, Ohio, Feb. 1968 (Contract AF33(615)-2862).
21. M. L. Hammond, P. F. Lindquist, and R. H. Bragg, "Structure of Vapor-Deposited Boron Filaments," AFML-TR-66-358, Air Force Materials Laboratory, W-PAFB, Ohio, Nov. 1966.

<u>Run #</u>	<u>Variables</u>	<u>Maximum Diameter</u>		<u>U.T.S.</u>		<u>E</u>	
		<u>mils</u>	<u>microns</u>	<u>psi</u>	<u>N/cm²</u>	<u>psi</u>	<u>N/cm²</u>
1 - 3	Hydrocarbon atmos., Subs. W 1.0 mil (25μ)	10.7	272.0	13,000	9,000		
4	subs. W 0.5 mil (12μ)	4.6	117.0	8,400	5,700		
5 - 9	Hydrocarbon & free radical sink	9.6	244.0	65,000	44,000	15-18 x10 ⁶	10-12 x10 ⁶
10 - 14	Subs. W 1.0 mil (25μ)	3.6	91.4	51,000	35,000		
15 - 21	Heating current, Subs. W 0.5 mil (12μ)	2.6	66.0	65,000	44,000		
30 - 43	Heating current	1.6	40.6	180,000	124,000		
44 - 60	Subs. C 1.0 mil (25μ)	1.8	45.7	105,000	72,300		
61 - 69	Hydrocarbon & boron	3.4	86.4	100,000	68,900		
107 - 115	Hydrocarbon & free radical sink, Subs. C 1.26 mil (33μ)	2.25	57.1	164,000	113,000		
116 - 123	Hydrocarbon & boron, Subs. C 1.3 mil (34μ)	3.8	96.5	271,000	186,000		
126 - 130	Do	3.6	91.4	244,000	167,000	20x10 ⁶	14x10 ⁶
131 - 146	Subs. C 1.27 mil (32μ)	7.0	178.0	224,000	155,000		
147 - 183	Subs. C 1.31 mil (33μ)	3.96	101.0	244,000	168,000		
184 - 205	Subs. C 1.34 mil (34μ)	4.09	104.0	417,000	285,000	29x10 ⁶	20x10 ⁶

APPENDIX

<u>Run #</u>	<u>Variables</u>	<u>Maximum Diameter</u>		<u>U.T.S.</u>		<u>E</u>	
		<u>mils</u>	<u>microns</u>	<u>psi</u>	<u>N/cm²</u>	<u>psi</u>	<u>N/cm²</u>
206 - 211	Heating current	3.93	100.0	311,000	213,000		
212 - 225	Heating current	5.5	140.0	370,000	255,000		
226 - 250	Subs. C 1.29 mil (33 μ)	3.95	101.0	421,000	290,000	28x10 ⁶	19x10 ⁶
251 - 367	Heating current	3.74	95.0	443,000	309,000	28x10 ⁶	19x10 ⁶